Interpretation of the lead isotopic composition from sulfide mineralizations in the Proterozoic Sjangeli area, northern Sweden

ROLF L. ROMER

Cu-, Fe-, and Zn-mineralizations occur in the Lower Proterozoic supracrustal rocks of the Sjangeli area, a tectonic basement window in the Caledonides of northern Sweden and Norway. The supracrustal belt consists of basic and ultrabasic metavolcanites which are intercalated with quartz-mica schists and banded carbonate-silicate rocks. The metavolcanites consist of tuffs, lava flows, and pillow lavas. Cu-mineralizations, which form three different types, occur within basic metatuffs. Two types represent epigenetic remobilizations of Cu-mineralizations, while the third type is characterized by stratiform bornite-chalcocite-quartz-magnetite layers of possible syngenetic origin. The Fe- and Zn-mineralizations occur in quartz-mica schists and form stratiform lenses.

At about 430 My a disturbance of the lead isotope system occurred, which changed the $^{238}U/^{204}Pb$, $^{232}Th/^{204}Pb$, and $^{232}Th/^{238}U$ ratios. Radiogenic lead was added to the mineralizations during the 430 My disturbance. The added lead component was different for the various deposits. Further, during the 430 My event, U was mobile, which is illustrated by the significantly increased $^{238}U/^{204}Pb$ ratios of the massive pyrrhotite mineralizations.

Lead lines from the recalculated lead composition (430 My) indicate mixing model ages of 1546 My to 2112 My. Since the mixed lead components were non-cogenetic, the model age variation of the mixing lines indicates differences of the mixing component, rather than real age differences. However, a lead source of Middle Proterozoic age can be deduced.

The Middle Proterozoic disturbance resulted in the formation of vein mineralizations which have predominantly high-uranogenic, low-thorogenic lead. The in-situ lead growth indicates high $^{238}U/^{204}Pb$ ratios and implies that U had also been mobile during the Proterozoic metamorphism.

Model ages for the least radiogenic lead (Kopparåsen) yield a minimum age of 2050 My.

R.L. Romer, Department of Economic Geology, University of Technology Luleå, S-951 87 Luleå, Sweden.

Introduction

In the southwestward younging Baltic Shield of northern Scandinavia (Skiöld 1986, 1987, Gaál & Gorbatschev 1987), the Rombak-Sjangeli basement window forms an accretionary zone of the Archean craton of probable island arc setting (Korneliussen et al. 1986). The Rombak-Sjangeli window is characterized by N-S striking volcano-sedimentary belts. The volcanites vary from basic and ultrabasic composition at the eastern border to intermediate and acidic composition in the west (e.g. Korneliussen et al. 1986). The Sjangeli area represents the easternmost of these Lower Proterozoic supracrustal belts and consists of basic volcanites (tuffs and lavas) and carbonate and pelitic sediments.

These Proterozoic supracrustal belts of the Rombak-Sjangeli window became intruded by acid to basic rocks at about 1700—1800 My ago. This is illustrated by Rb-Sr ages deduced from whole-rock isochrons from granites, e.g. 1691 ± 90 My (Heier & Compston 1969) and 1780 ± 85 My (Gunner 1981). Subsequently, the Proterozoic rocks were eroded and were covered by discontinuous metaconglomerates and arkosic quartzites (cf. Kulling 1964, Tull et al. 1985), presumably during the Cambrian (Bergström & Gee 1985). The quartzites generally form thin flat-lying veneers, but locally they are bent upright along steep faults which remobilized basement blocks (Bax 1986, 1989). The basement reactivation is related to the Caledonian overthrusting, which in the Rombak-Sjangeli area probably started about 450 My ago (e.g. Tull et al. 1985). The overriding of the Caledonian nappes over the basement resulted in a low-grade metamorphism reaching greenschist facies (e.g. Bryhni & Andre-
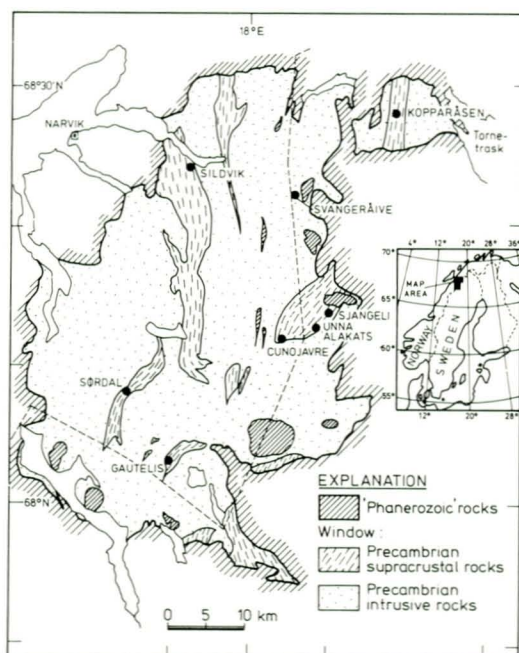
Fig. 1. Simplified geologic map of the Rombak-Sjangeli basement window (after Vogt 1950, Kulling 1964, Romer 1987). Sample (Table 1) locations are indicated. For more detailed information about the sample locations in the Sjangeli area see Fig. 2 and Romer (1987).
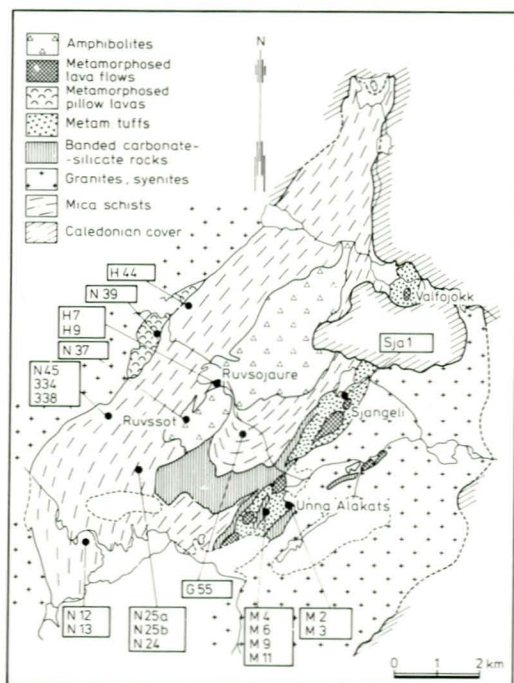

Fig. 2. Simplified geologic map of the Sjangeli supracrustals (after Romer 1987), showing the distribution of the volcanic units and the sample locations.

asson 1985, Tull et al. 1985) in the eastern part of the basement windows, which includes the Sjangeli area.

Sulfide mineralizations occur within the supracrustal belts of the Proterozoic basement. The lead isotopic composition of sulfide minerals from some of these mineralizations (cf. Figs. 1 & 2) has been determined. The bulk of these analyses comes from the Cu-mineralizations of the Sjangeli area and their wall rocks.

The purpose of this paper is (1) to use the lead isotopic composition of the samples to illustrate the effect of the Caledonian and Svecokarelian orogenies on the isotopic composition of the sulfide lead and the whole-rock trace lead; and (2) to use the lead composition as a tracer of the source of the different lead components.

Geology of the Sjangeli area

The Sjangeli supracrustal belt lies at the eastern border of the Rombak-Sjangeli window

(Fig. 1) and is correlated with the Kopparåsen and the Gautelis supracrustal rocks (cf. Adamek 1975, Romer 1987). The Sjangeli supracrustal belt, which is about 10 km long and reaches a width of 5 km, strikes approximately N-S and the units dip steeply to the west (70-85°). The belt is characterized by a strike-parallel 'zebra-stripe' pattern consisting of volcanic units which are intercalated with sedimentary and volcano-sedimentary units.

To the east (Fig. 2), the metamorphosed volcanic rocks are lava flows, that are embedded in basic metatuffs, and which commonly are strongly mylonitized. The lava flows occur only in this easternmost volcanic unit, and they do not contain any mineralizations. The waterlain basic metatuffs, hereafter sometimes simply called tuffs, contain thin layers of banded silicate-carbonate rock. The tuffs are the most intensely mineralized part of the Sjangeli area. Most of the stratabound mineralizations are stratiform, but locally discordant quartz-bornite veins also occur, which could represent remobilizations of stratabound mineralizations.

The central volcanic unit consists of high-Mg basalts (12-18 % MgO) which contain lenses of serpentinites. The amphibolites consist mainly of layered metatuffs, but locally contain pillow lavas and thin layers of banded carbonate-silicate rock. The high-Mg basalts have high contents of Cr and Ni (Romer 1987) and show platinum group element ratios similar to komatiites (Barnes et al. 1988). The amphibolites do not contain Cu-mineralizations. A metasomatic alteration zone which contains a magnetite layer with bornite occurs at the NE contact between the mica schists and a serpentinite lense.

The western volcanic unit consists of pillow lavas which locally are interlayered with thin discontinuous layers of banded carbonate-silicate rock. This unit does not contain Cu-mineralizations.

Quartz-mica schists and banded silicate-carbonate rocks intercalate with the volcanic and volcano-sedimentary units. At Ruvssot (Fig. 2) the quartz-mica schists contain stratiform Cu-mineralizations in the vicinity of the metasomatized alteration zone of the amphibolites. The quartz-mica schists contain additional stratiform Fe-mineralizations and at Cunojavre (cf. Fig. 2) they contain a stratiform Zn-mineralization.

The amphibolites show Early Proterozoic amphibolite facies mineral assemblages. The other volcanic units have been extensively retrograded and show greenschist facies mineral assemblages.

Two metamorphic events and possibly the spilitization of the volcanic rocks have disturbed the isotope systems. The youngest event, which partially reset the isotope systems, is the Caledonian orogeny. Here, the term Caledonian is used rather loosely and refers to any event in the approximate time range 380 to 480 My. Rb-Sr whole-rock data yield mixing lines with an apparent age of 488 ± 64 My (Romer 1989). Similarly, mineral Rb-Sr isotope data indicate a partial remobilization of the isotope systems at that time. Since the mixing lines do not yield ages, no precice time constraints for the Caledonian overthrusting can be deduced for these lines. Tull et al. (1985) refer to a dynamometamorphic event prior to c. 450 My ago to the west of the Rombak-Sjangeli area, while mineral ages from Vestvågøy vary from c. 460 My (amphiboles) to c. 350 My for bictites (Tull et al. 1985). For the recalculation of the lead isotope composition, an age of 430 My was arbitrarily chosen.

Whole-rock lead lines indicates ages of 1600 - 1800 My (Romer 1989). These ages coincide with the ages of the Svecokarelian granites, to which the granites and syenites of the Rombak-Sjangeli window belong (cf. Gorbatschev 1985). Similar metamorphic ages were obtained for the Vesterålen area (e.g. Griffin et al. 1978, Jacobsen & Wasserburg 1978).

Rb-Sr whole-rock data yield a date of 2324 ± 15 My (Romer 1989). Since this date is based on only 3 analyses and as the area has been metamorphosed twice, it probably does not represent a reliable age and is probably too high by 100 to 150 My (cf. Romer 1989). Ages in excess of 2000 My have been reported from the Vesterålen area (Griffin et al. 1978). Where metavolcanites yield ages of about 2200 My.

Mineralization types

In the Sjangeli area, mineralizations of Cu, Fe, and Zn predominately form stratiform lenses and layers. However, Cu-mineralizations also form remobilizations in discordant veins and metasomatized contact zones. In the following discussions, the mineralizations are classified according to their main metal and, in addition, the Cu-mineralizations are classified into types (i), (ii), and (iii), while the Fe-mineralizations are separated into magnetite and pyrrhotite mineralizations.

Cu-mineralizations occur within the basic tuffs at Unna Alakats, Sjangeli, and further to the north at Valfojokk (Fig. 2). Comparable Cu-mineralizations occur in similar wall-rock at Ruvsojaure and in the quartz-mica schists at Ruvssot. In addition, Cu-mineralizations at Ruvssot are related to a magnetite band in the metasomatic alteration zone between the ultrabasic volcanites and the mica schists (Fig. 2).

The Cu-mineralizations form three main types, that differ in respect to the field occurrence and the main copper sulfide (Romer 1987):

Type (i) is the predominate mineralization in the Sjangeli area. It forms massive bands and lenses that contain more than 50% sulfides and oxides, with sulfides dominating over oxides. The bands are up to 5 cm broad and up to 50 m long while the lenses have a length of 20 to 50 cm and are 2 to 5 cm thick. The

bands and lenses contain mainly bornite, chal-
cocite and magnetite. Epidote and quartz are
the main gangue minerals, while Fe-actinolite
is minor.

Type (ii), which is only found at Unna Ala-
kats, forms schistosity-parallel quartz veins
which are discordant to the bedding. The qu-
artz veins, about 5 cm broad, are paralleled by
a sulfide band on one or both sides. The sulfi-
de bands contain bornite and chalcocite toget-
her with minor magnetite. These bands were
probably formed during the Proterozoic meta-
morphism and deduced their metal content
from preexisting mineralizations of type (i).

Type (iii) occurs at Ruvsojaure and is diffe-
rent from the other two types since bornite
and chalocite are absent and chalcopyrite al-
most exclusively occurs in small veins. The
mineralization is bound to an intensely epidoti-
zed and partly actinolitized amphibolite, which
resembles the basic metatuffs from Unna Ala-
kats.

In addition to these three main types (i-iii),
a 1-3 m thick, 100 m long magnetite zone
with abundant bornite occurs at Ruvssot. This
zone is part of the metasomatic alteration
zone between the serpentinites and the quartz-
mica schists (Romer 1987).

Within the mica schists, banded quartz-
magnetite mineralizations form stratiform bodi-
es up to 1 m thick and 40 to 60 m long. Poly-
crystalline 'globules' of coarse pyrite and chal-
copyrite, about 1 cm in diameter, occur local-
ly within the magnetite bands. Near Cunojavre
a stratiform Zn-mineralization, about 100 m
long, forms a thin (5-10 cm) schistosity-concor-
dant 'sheet'. Sphalerite is the main mineral
of this massive mineralization, but minor pyrr-
hotite, chalcopyrite and pyrite also occur. Furt-
her, within the amphibolites, a 50 m long, 5-30
cm broad stratiform pyrrhotite mineralization
occurs, consisting exclusively of pyrrhotite and
quartz.

Methods

All isotope measurements were performed
during a research visit at the University of
California, Santa Barbara. Ion exchange techni-
ques were used to separate Pb, U, and Th
(Grünenfelder et al. 1986). Contents of Pb, U
and Th were determined by isotope dilution
using a composite ^{208}Pb-^{235}U-^{230}Th tracer. Pb
was measured using a Re single filament sili-

ca-gel technique (e.g. Cameron et al. 1969) on
a Finnigan MAT 261 multi-collector mass spect-
rometer. The Pb mass fractionation correction
factors were calculated for NBS 981 Pb-
standard, using $^{208}Pb/^{206}Pb$ = 2.16715 (Todt et
al. 1984). The lead composition was measured
with a 2σ precision better than $\pm$ 0.08% ($^{206}Pb/$
^{204}Pb). U and Th were measured on an AVCO
single collector solid source mass spectrome-
ter, using a Re single filament 'carbon sand-
wich' technique (HNO-load of U and Th bet-
ween two carbon layers; G.R. Tilton, pers.
comm.). Uncertainties in the concentration
data are c. 0.3% for Pb and 1% for U and Th.

The decay constants recommended by Stei-
ger & Jäger (1977) were used.

Sample description and results

The lead compositions of sulfide concentrates
from mineralizations in the Sjangeli area and
the Rombak-Sjangeli window are reported in
Table 1. The locations of the samples are indi-
cated in Figs. 1 & 2.

Sample M11 belongs to the Cu-mineralizati-
ons of type (ii), while all other Mx samples
and sample Sja-1 belong to the Cu-mineralizati-
ons of type (i). Samples M2 and M3 originate
from the same mineralization. Sample M3
comes from the massive, central part of the
mineralization, while M2 comes from a less
mineralized section. Samples M4 and M6 are
disseminated sulfides from the wall rock of
massive mineralizations, and samples M9 and
Sja-1 come from massive mineralizations.
Samples H7 and H9 are from Cu-mineralizati-
on type (iii) from Ruvsojaure.

Three sulfide concentrates from the pyrite-
chalcopyrite 'globules' from the magnetite
mineralization have been analyzed (N45, 334,
338). Samples N24, N25a, and N25b originate
form the pyrrhotite mineralization. Pyrrhotites
N25a and N25b come from the same speci-
men; however, pyrrhotite N25b is more strong-
ly magnetic than pyrrhotite N25a. Sample N37
was obtained from the bornite-mineralized
magnetite band in the above-mentioned meta-
somatized alteration zone at Ruvssot.

Samples H44 and G55 are from impregnati-
ons in the quartz-mica schists, while samples
N12 and N13 are from massive mineralizations.

Lead isotope data have also obtained from
the various igneous (now metamorphosed)

Sulfides from the Sjangeli area

Cu-mineralizations

sample	mineral	$^{206}/_{204}$	$^{207}/_{204}$	$^{208}/_{204}$	Pb	U	Th
H7	py	44.485	18.579	37.391	2.3	.87	.107
H9	py	119.28	29.579	41.174	6.1	—	—
M2	py	18.730	15.616	39.426	5.2	.017	.05
M3	py	15.911	15.269	35.923	62.	0.0033	.0038
M4	bo+cct	31.571	17.240	48.356	3.9	.018	.007
M6	bo+cct	36.699	17.428	47.466	5.	—	—
M9	py+bo+cct	37.397	17.900	38.822	4.1	.064	.017
M11	py+ccp	22.899	16.059	39.924	9.7	.026	.023
Sja-1	bo+ccp	25.428	16.448	40.470	9.9	.55	.0005

Fe-mineralizations

sample	mineral	$^{206}/_{204}$	$^{207}/_{204}$	$^{208}/_{204}$	Pb	U	Th
N24	po	38.038	17.760	44.091	2.0	1.43	.33
N25a	po	24.284	16.229	39.270	3.9	2.88	.23
N25b	po	34.014	17.405	43.635	4.	.24	.073
N37	sph	25.703	16.509	42.644	6.66	.069	.065
N45	py	18.285	15.607	36.885	8.9	.046	.025
334	py+ccp	22.804	16.159	40.920	3.5	—	—
338	py	28.621	17.105	43.312	1.6	.024	.027

Zn-mineralizations

sample	mineral	$^{206}/_{204}$	$^{207}/_{204}$	$^{208}/_{204}$	Pb	U	Th
N12	po	23.607	16.162	41.759	999.0	.082	.126
N13	sph	26.962	16.559	41.632	10.0	.042	.048

Other mineralizations

sample	mineral	$^{206}/_{204}$	$^{207}/_{204}$	$^{208}/_{204}$	Pb	U	Th
G55	asp	16.578	15.368	36.233	4.4	.215	.245
H44	py	17.489	15.519	36.369	5.8	.02	.029

Sulfides from other supracrustal belts in the Rombak-Sjangeli area

sample	mineral	$^{206}/_{204}$	$^{207}/_{204}$	$^{208}/_{204}$	Pb	U	Th
Kopparåsen	ga	15.293	15.192	35.083	—	—	—
Gautelis	asp	20.850	15.880	39.139	7.9	.18	.11
Sildvik	sph	15.765	15.311	35.483	14.3	.03	.053
Sørdal	py+ccp	19.756	15.690	37.292	3.7	—	—

Table 1. Lead composition and contents (in ppm) of Pb, U, and Th of sulfides from the Sjangeli and related areas. For sample location compare Figs. 1 & 2. py = pyrite; po = pyrrhotite; bo = bornite; sph = sphalerite; ga = galena; ccp = chalcopyrite; cct = chalcocite; asp = arsenopyrite.

rocks of the Sjangeli area. The whole-rock lead isotope data for the tuffs, the amphibolites, the lava flows, and the granites is presented in Romer (1987, 1989).

Since most samples contained only trace lead (0.6-62 ppm Pb) and also contained traces of U and Th (up to 2.9 ppm U and 0.33 ppm Th; see Table 1), the lead compositions

have been altered by in-situ radiogenic lead generation. To obtain the lead composition at the time of the last disturbance, the lead has to be recalculated based on the assumption that the contents of U, Th and Pb remained unchanged after the last event. The time for recalculation was arbitrarily set to 430 My (see also the section on the geology of the Sjangeli area). The recalculation eliminates the effect of in-situ radiogenic lead addition, and mixing relationships should become more obvious. Note that the recalculation of the isotopic composition of the lead is based on the assumption of no gain/loss of U, Th, and Pb.

The isotopic composition of the sulfide lead at 430 My

The sulfide lead isotopic compositions, shown in Fig. 3, form a rather well defined linear array in the $^{206}Pb/^{204}Pb$ - $^{207}Pb/^{204}Pb$ plot. However, in the $^{206}Pb/^{204}Pb$ - $^{208}Pb/^{204}Pb$ diagram, the samples scatter, and there are samples with high $^{206}Pb/^{204}Pb$ ratios and anomalously low $^{208}Pb/^{204}Pb$ ratios (e.g. H7, M9). The lead isotopic composition of the Fe-mineralizations and the Cu-mineralizations differs (cf. Fig. 6). There are also differences between the various Cu-mineralizations and, further, between the magnetite and the pyrrhotite Fe-mineralizations.

The Cu-mineralizations define a single lead line in the $^{206}Pb/^{204}Pb$ - $^{207}Pb/^{204}Pb$ diagram, while in the $^{206}Pb/^{204}Pb$ - $^{208}Pb/^{204}Pb$ diagram two different lead trends are obvious. One trend, defined by most Mx samples and Sja-1 shows a $^{208}Pb/^{206}Pb$ ratio of about 0.75, while the second trend defined by Hx and M9 falls clearly below this trend (cf. Fig. 3).

Samples H7 and H9 belong to the mineralizations of type (iii), while M9 belongs to mineralization type (i). Lead from these Cu-mineralizations indicates a lead growth in a high μ ($^{238}U/^{204}Pb$), low ω ($^{232}Th/^{204}Pb$) environment.

In contrast to these samples, samples from mineralization type (i) (except M9) show a highly variable lead composition, with low radiogenic lead for massive mineralizations and with more radiogenic lead in low-grade (usually disseminated) mineralizations. The radiogenity of the lead composition of this type correlates negatively with the lead contents (cf. Fig. 4) and therefore the lead line of the type (i) mineralizations could be the result of isotopic mix-
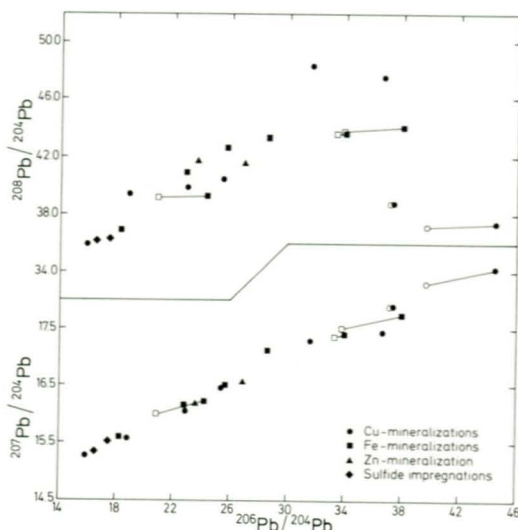

Fig. 3. Lead isotope ratios from sulfides from the different mineralization types of the Sjangeli area. Recalculated isotopic compositions for 430 My (open symbols) are also shown if the recalculated and measured ratios differ beyond drafting resolution. Tie-lines connect the recalculated and the measured composition. Regression lines for the various mineralization types are used to calculate model ages and apparent ratios (see Table 2).
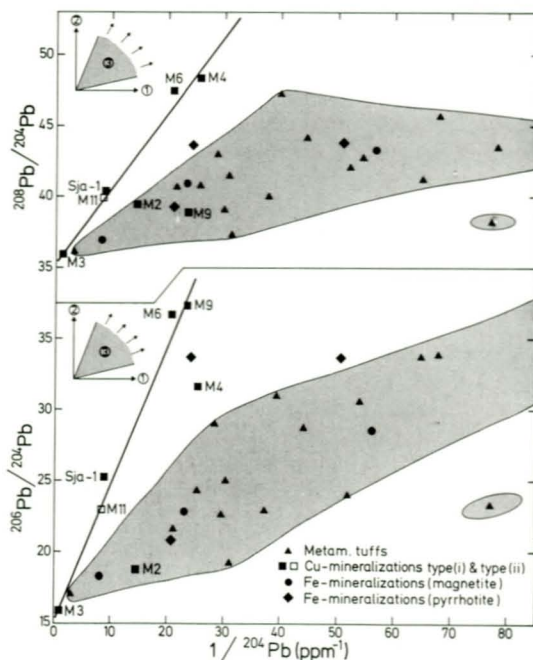

Fig. 4. $^{206}Pb/^{204}Pb$ - $1/^{204}Pb$ and $^{208}Pb/^{204}Pb$ - $1/^{204}Pb$ mixinf plit for lead compositions recalculated to 430 My (except for the open symbols, which represent present-day lead). Trace lead data from sulfides of Cu- and Fe-mineralizations are recalculated from Table 1. The data for the tuffs are recalculated from Romer (1987).

Fig. 5. Lead isotope ratios from different units from the Sjangeli area (recalculated for 430 My). Data from Table 1 and Romer (1987). For discussion see text.
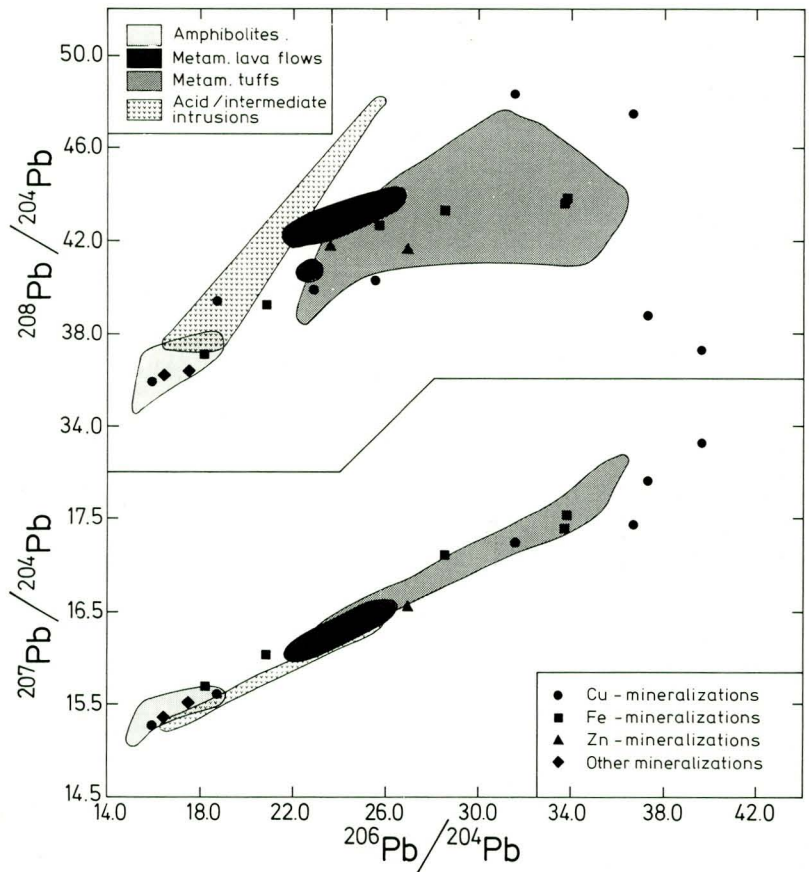

ing of two isotopically different lead compositions. This would explain the constant κ ratio (^{232}Th/^{238}U) necessary to obtain a linear trend in the ^{206}Pb/^{204}Pb - ^{208}Pb/^{204}Pb diagram. Further, there would be no need for a negative correlation between the isotopic ratios and the lead contents, as an in-situ lead growth interpretation would imply (since lead content and lead radiogenity correlate negatively, cf. Fig. 4). The slope of the tie-line of samples M2 and M3 reflects a higher ^{208}Pb/^{206}Pb ratio than all other trends (Fig. 3). This indicates that if there had been mixing, the mixing lead composition cannot have been completely homogenous. The added lead composition, which could have been introduced at different times near 430 My, must have had local variations in its isotopic composition. Sample M11, which is the only sample from Cu-mineralization type (ii), falls on the trend defined by samples from Cu-mineralization type (i).

The lead composition from the Fe-mineralizations differs widely. Sulfide lead from the magnetite mineralizations follows the same trend as the Cu-mineralization type (i) lead. However, the lead from the magnetite mineralizations has a higher ^{207}Pb/^{204}Pb ratio for a given ^{206}Pb/^{204}Pb ratio (cf. Fig. 6). The pyrrhotite lead from the pyrrhotite mineralization is characterized by a large in-situ decay correction, since pyrrhotite has large contents of U. Note that the pyrrhotite has rather low Th contents. The lead line through the recalculated samples has a flatter slope in the ^{206}Pb/^{204}Pb - ^{207}Pb/^{204}Pb and the ^{206}Pb/^{204}Pb - ^{208}Pb/^{204}Pb diagram than the type (i) Cu-mineralizations and the magnetite mineralizations.

The recalculation of the pyrrhotite lead (N24, N25, N25b) to 430 My aligns all three samples along a straight line, which has a different slope than the in-situ decay correction tie lines, indicating that after 430 My the lead evol-

Fig. 6. Sulfide trace lead isotope ratios from minerali- zations from the Rombak- Sjangeli basement window (Fig. 1) and the Nasafjæll window. The ratios are re- calculated for 430 My, ex- cept for the open symbols. For comparison, the field defined by the lead compo- sitions of samples from the Sjangeli area (Fig. 5) are shown.
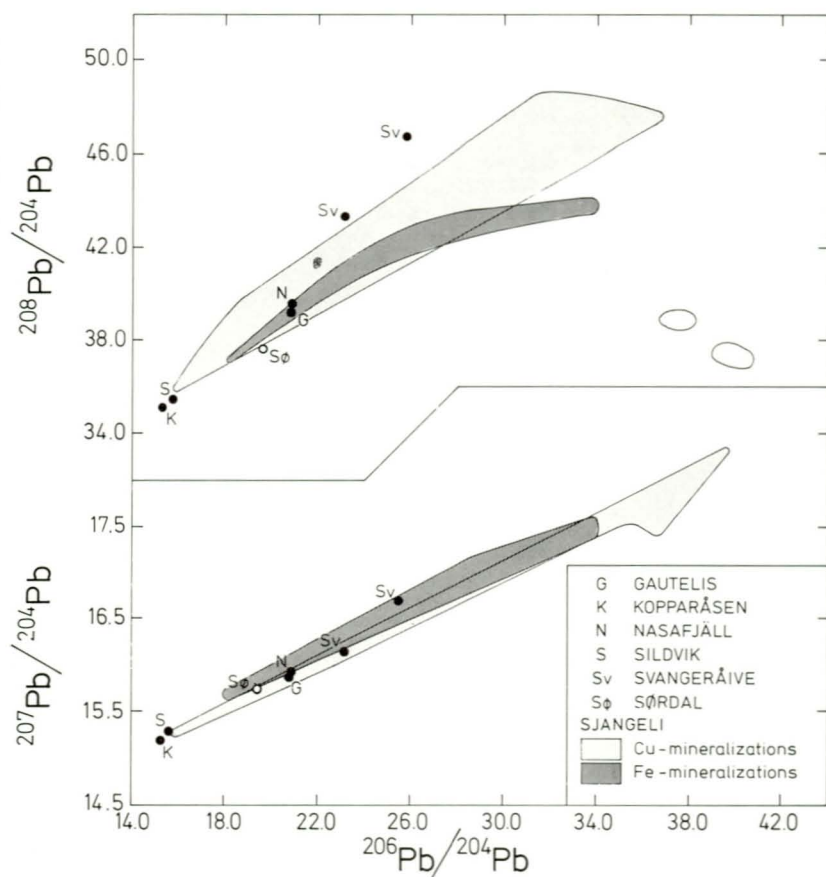
ved with different μ and ϖ ratios. The 430 My line between the different pyrrhotite samp- les could be a mixing line between a primary low radiogenic lead composition, possibly simi- lar to N25a, and a more radiogenic lead. Asso- ciated with such a mixing, U could have been introduced into the pyrrhotites. This mixing process would provide a mechanism to selecti- vely add U and Pb to the pyrrhotite.

The lead composition of the Zn-mineralizati- on is highly radiogenic although both samples (N12 and N13) come from a massive minerali- zation and have high Pb contents. In addition, tne tie-line of the two samples N12 and N13 has a flat, negative $^{208}Pb/^{206}Pb$ slope. This sug- gests that the lead of the Zn-mineralizations represents a mixture of two non-cogenetic lead components.

The isotopic composition and source of the 'contamination' lead

The recalculated lead compositions of sulfides from the different mineralizations fall on diffe- rent linear trends (Fig. 3; $^{206}Pb/^{204}Pb$ - $^{208}Pb/^{204}Pb$ diagram). If these lines represent mixing lines, this demonstrates that there is no common mixing component. Since these mineralization types are geographically separated and some of them are related to different lithologies (cf. Fig. 2), it is possible that the lead of the host- rocks has contributed to the mixing lead, which would give the mixing lead a local modi- fication and variation.

For example, the lead composition of the type (i) Cu-mineralizations and their host- rocks, the tuffs, plot in fields which overlap (cf. Fig. 5). However, for the same $^{208}Pb/^{204}Pb$ ratio the tuffs have a wider variation of the $^{206}Pb/^{204}Pb$ ratio and usually also have higher $^{206}Pb/^{204}Pb$ ratios.

The sulfide lead composition could be ex- plained with a simple two component mixing process. One lead component would have a low radiogenic lead composition, similar to sample M3 or the Kopparåsen galena, while the other lead component has to be more radiogenic than sample M4 or M6. Setting

^{206}Pb/^{204}Pb arbitrarily to 38.0, the other ratios are fixed at ^{207}Pb/^{204}Pb = 18.06 and ^{208}Pb/^{204}Pb = 50.0 (cf. Fig. 3). Such an end member could also partially explain the variation of the lead composition of the tuff lead composition. The remaining lead variability of the tuff lead composition would be due to another lead component, which formed in a low κ environment, or would be due to in-situ lead growth in a low κ environment. The ^{206}Pb/^{208}Pb ratio of such a lead component would indicate a potential source with an average Th/U atomic ratio of about 2.85 for the time interval from 1800 My to 430 My.

Alternatively, the lead variation of type (i) Cu-mineralizations could be due to accumulation of lead which was leached from the immediate wall rock. If the wall rock of all type (i) mineralizations had the same ratio, then the mixing with a highly variable lead extracted from the wall rock still yield a linear sulfide lead trend. If sulfides and the wall rock once had the same isotopic composition, then the mixing line would represent the time of isotopic homogenization of sulfides and wall rock, i.e. it would represent the time of formation or the time of a metamorphic homogenization. The anomalous widening of the metatuff lead composition field for more radiogenic lead in the ^{206}Pb/^{204}Pb - ^{208}Pb/^{204}Pb diagram could be due to the addition of low ϖ lead, or a negative correlation of μ and κ.

This is compatible with the observation that the whole-rock lead composition usually is more radiogenic than the lead composition of the coexisting sulfides. The sulfides could represent a mixture of a low radiogenic lead component and a radiogenic lead component which was derived from wall rock leaching at about 430 My.

These two models can be tested in mixing diagrams (fig. 4). The sulfide samples from the type (i) Cu-mineralizations yield a good linear alignment in both mixing diagrams, ^{206}Pb/^{204}Pb - 1/^{204}Pb [ppm-^{1}] and ^{208}Pb/^{204}Pb - 1/^{204}Pb [ppm-^{1}]. The sulfide data could therefore be explained with simple mixing.

However, the tuff lead composition is not compatible with such a simple mixing. The mixing trend in the ^{206}Pb/^{204}Pb - 1/^{204}Pb [ppm-^{1}] diagram is scattered and delineates a field rather than a straight line. This field shows a negative correlation between the ^{206}Pb/^{204}Pb ratio and the ^{204}Pb content. In the ^{208}Pb/^{204}Pb - 1/^{204}Pb [ppm-^{1}] diagram, the tuffs form a wide

sub-horizontal field (Fig. 4). The ^{208}Pb/^{204}Pb ratio does not vary systematically with the ^{204}Pb content of the samples, and therefore, there has been no mixing or the mixing component did not contain ^{208}Pb. Alternatively, if all the metatuffs had been enriched in U for a long time, then the variation in radiogenity of the tuffs is mainly due to variable μ ratios for the different samples. However, to obtain a linear field (in Fig. 4), there should be at least a weak correlation between μ and ^{204}Pb ppm. Assuming a homogeneous lead composition of the tuffs at the time of infiltration and no external lead addition, the slope of the tuff field in the ^{206}Pb/^{204}Pb - ^{207}Pb/^{204}Pb diagram (Fig. 3) indicates a model age of 1910 My.

The obvious contrast between the sulfide lead and the tuff lead in the mixing diagrams (cf. Fig. 4) probably indicates a differential acceptance of externally added lead in the sulfides and in the whole-rock sample. If only the sulfides received externally derived lead, while the silicates of the whole-rock samples did not accept additional lead, then the sulfide lead would show mixing lines, while the silicate lead would show in-situ lead growth. Since the tuffs also contain a minor amount of sulfides, they would, according to the above reasoning, also have obtained an external lead addition, although only a minor one. However, for this model, the metatuff lead line has no strict age meaning, since there is an external, probably non-cogenetic lead component present.

The Fe-mineralizations also yield linear trends which could be interpreted as mixing lines. However, they received an isotopically different lead component (cf. Fig. 3).

Lead from a low κ source

If an oxidized fluid infiltrates a permeable rock which reduces the fluid, then the U in the fluid would precipitate. Such a process could have caused the U enrichment of the tuffs, the selective U enrichment of the pyrrhotite mineralizations and the pyrites of sample H7 (cf. flat 0-430 My tie lines in the ^{206}Pb/^{204}Pb - ^{208}Pb/^{204}Pb diagram Fig. 3).

For the metatuffs, such an U infiltration would have happened about 1600 - 1800 My ago, probably in connection with the Svecokarelian metamorphism and the intrusion of the Proterozoic granites and syenites into the Rombak-Sjangeli supracrustal rocks.

The infiltration of U into the pyrrhotite mineralization, however, happened about 430 My ago (cf. Fig. 3 and section on 430 My lead composition). The pyrrhotite line in Fig. 3 could represent a mixing line similar to the magnetite mineralization line and the type (i) Cu-mineralization line. However, in a mixing diagram (Fig. 4) the pyrrhotite points do not form a line. Since the primary lead contents of samples could have been different, this does not necessarily rule out mixing. The pyrrhotite line yields a model age for cogenetic lead of 1550 My and an apparant κ ratio of 1.22. The slope of the pyrrhotite line in the $^{206}Pb/^{204}Pb$ - $^{208}Pb/^{204}Pb$ diagram (Fig. 3) indicates lead growth in an environment with a higher ratio than after the U addition.

Cu-mineralizations of type (ii) and type (iii) are characterized by low κ lead. Since these mineralizations do not contain high κ lead and the possible mixing components, which have been recognized, have developed in a high κ environment, it is suggested that these mineralizations are older than the mixing event at about 430 My. These mineralization types (ii and iii) could have formed during the same event which caused the U infiltration into the tuffs. If they had acquired a high μ ratio at the same time, their low κ lead could be due to in situ lead growth.

The isotopic composition and source of the 'primary' lead

The most primitive lead composition found in the Sjangeli area was found in sample M3. However, in the northward continuation of the Sjangeli area, the Kopparåsen area, galena with a less radiogenic isotopic composition has been found. This galena lead falls on the same lead line as the type (i) Cu-mineralization lead, and probably represents an uncontaminated lead composition. Alternatively, the more radiogenic character of M3 could be explained by a complete or partial homogenization of the sulfide lead with its surrounding whole-rock at about 1600 - 1800 My.

Model ages for the galena lead composition vary from 1950 My (Stacey & Kramers 1975) to 2050 My (Zartman & Doe 1981). In a Zartman & Doe (1981) model, the galena lead would represent a mixture of lower crust lead with upper crust lead at about 2050 My. However, the galena composition could also be

modelled with a mixture of an old lower crust lead and a younger upper crust lead. In this case, the older component could have preserved its low radiogenic composition as galena, from the time of separation to the time of mixing. At the time of mixing, this old lead would have mixed with a younger lead component. Using a upper crust lead of 1600 My age, the corresponding lower crust lead would have an age of more than 2200 My. For this model, the galena lead composition would give a minimum model age of the supracrustal rocks. Note that such model ages rely on the correctness of the model, and could yield model ages considerably higher than indicated by other methods (e.g. Vaasjoki 1981, Sundblad & Røsholt 1986).

The lead isotope constraints on the alteration of the Sjangeli mineralizations

From the mixing lines and mineral tie lines (0 - 430 My) in Fig. 3, model ages can be calculated. These model ages are based on the assumption of cogenetic mixing components. The same assumption also allows for the calculation of an apparant ratio for the time from the separation of the two lead reservoirs to the time of mixing. The mineral tie lines reflect the in-situ κ ratio which also can be calculated from the U and Th contents in Table 1. These model parameters are summarized for the various mineralization types in Table 2.

The variation of the model ages represents the effect of a variable non-cogenetic mixing component instead of different ages. However, the consistency of the model ages indicates that the source rocks probably were of Early to Middel Proterozoic age. Alternatively, there could have been an Early to Middle Proterozoic 'homogenization' event, during which the lead of the mineralizations and the source rocks of the 430 My lead homogenized. Both explanations are compatible with a Svecokarelian orogeny with the intrusion of granites and syenites (cf. Heier & Compston 1969, Gunner 1981, Gorbatschev 1985) and related metamorphism.

A comparison of the pre-mixing and post-mixing ratios shows a strong decrease for the pyrrhotite and probably the type (ii) Cu-mineralizations. This indicates that for these minerali-

	model mixing age	pre-mixing κ	post 430 My κ	model time of U/Th separation	
Cu-type (i)	1630	2.05	0.27-3.02	—	
Cu-type (ii)	1630(?)	2.05(?)	0.91	—	
Cu-type (iii)	(2040)	(0.17)	0.056	1600-1800	430?
Fe magnetite	2110	2.15	0.56-1.15	—	
Fe pyrrhotite	1550	1.22	0.078-0.245	430	
Zn	1700	—	—	?	

Table 2. Model mixing ages and apparent pre-mixing k (for a homogenization time of 1700 My) calculated from the data in Table 1 and fig. 3. Note that the model mixing ages and the apparent k ratios assume cogenetic mixing lead components. The post-mixing (430 My) ratios are calculated from Table 1. The model time of U/Th separation is estimated from changes in the lead growth trends at c. 430 My and c. 1800 My respectively. Values in parentheses (type iii) represent maximum model ages and minimum pre-mixing ratios (only one sample was recalculated). The type (ii) Cu-mineralization data in parentheses are inferred from type (i) Cu-mineralization data.

zations a separation of U and Th occurred at approximately 430 Ma. The contrast of solubility of U and Th in oxidized fluids (e.g. Boyle 1982) suggests a hydrothermal transport. The pre-mixing κ ratio indicates an upper crustal lead source, since other reservoirs have higher κ ratios, e.g. bulk Earth 4.2 (Allégre et al. 1986), lower crust ≈5.9 - 10 (Heier & Thoresen 1971, Dostal & Capedri 1978, Zartman & Doe 1981) and mantle ≈3 - 4 (Zartman & Doe 1981).

The anomalously low thorogenic lead composition at 430 My of the type (iii) Cu-mineralizations and the tuffs (cf. Figs. 3 & 5) indicates that there had been an earlier separation of U and Th, which was possibly related to the Svecokarelian metamorphism. This 1600 - 1800 My metamorphism probably represents the time of formation of the remobilized Cu-mineralizations of type (ii) and type (iii).

Indications that the metamorphic fluids were oxidized and could have transported U come from the chemical composition of epidotes from the tuffs and lava flows (cf. Romer 1987). Epidotes from the Sjangeli area have a $X_{pistacite} ≈ .33$, and indicate that they have equilibrated with an oxidized fluid (Bird & Helgeson 1981). In such a fluid, U is predominantly in the 6+ state (Langmuir 1978, Romberger 1984), and therefore mobile.

The lead compositions of the Cu-mineralizations and the Fe-mineralizations differ (Fig. 6). Since these two mineralization types are rela-

ted to different lithologies, the isotopic difference may indicate that there was some wall rock leaching or that the lead composition of the fluid was different in the various mylonitic zones.

No isotopic constraints can be given for the genesis of type (i) Cu-mineralizations, since there probably had been a rather extensive isotopic homogenization during the Svecokarelian orogeny. However, the stratiform nature and their selective occurrence in the tuffs indicates a possible syngenetic origin in a subaquatic shallow-water depositional environment. Such an environment is indicated by the occurrence of tuffs (Romer 1987) and lapilli (Adamek 1975) in the Kopparåsen area (see Fig. 1).

Comparison of other sulfide lead compositions with the Sjangeli sulfide lead

There are only a few lead isotope analyses available from other supracrustal units of the Rombak window. Samples from mineralizations have been provided by Are Korneliussen (NGU, Trondheim) from Sildvik and Sørdal and by Frank-Dieter Priesemann (Folldal Verk A/S, Folldal) from Gautelis. The other data consist of analyses from galena mineralizations from Svangeråive (Johansson 1983) and from Nasafjäll (Johansson 1983), a basement window about 300 km south of the Sjangeli area.

The limited amount of data from these supracrustal units (Table 1) does not allow for an equally thorough discussion of the data as for the Sjangeli area. Instead, these samples are compared with the sulfide samples from the Sjangeli area (Fig. 6).

(1) The lead composition of massive sulfide mineralizations from supracrustal belts within the Rombak-Sjangeli window show the same variation as the type (i) Cu-mineralizations of the Sjangeli area, and could therefore have been affected by similar processes. The Svangeråive samples (Johansson 1983), however, have significantly higher $^{208}Pb/^{204}Pb$ ratios at a given $^{206}Pb/^{204}Pb$ ratio, and further the $^{207}Pb/^{206}Pb$ ratios are slightly higher than for the type (i) Cu-mineralizations.

Johansson (1983) interpreted the lead composition of the Svangeråive deposit (20 km north of Sjangeli) as the result of the addition

of a preferentially leached, radiogenic, Karelian lead component. The lead isotopic composition of granites form the Sjangeli area shows the same thorogenic lead as the Svangeråive deposits (cf. Figs. 5 & 6), and therefore it is possible that lead leached from granites and syenites with a similar lead composition as the Sjangeli granites could have been involved in the formation of the Svangeråive galena mineralizations. However, if the lead composition of the leached lead and the old lead component were non-cogenetic, model ages such as c. 1970 My for Svangeråive and c. 1660 My for Nasafjäll (Johansson 1983) do not give the age of the source.

(2) The lead addition during the Caledonian metamorphism seems to be common for basement mineralizations throughout the entire Rombak-Sjangeli basement window. The degree of observed lead radiogeneity depends not only on the amount of circulating fluid and the effectiveness of lead precipitation, but also on the lead concentrations and the total amount of lead present in the mineralizations. The low radiogenity of lead from Kopparåsen and Sildvik may reflect that their original lead composition is less contaminated by a radiogenic lead component.

Conclusions

The trace lead of sulfides from Cu-, Fe-, and Zn-mineralizations from the Sjangeli area show at least two events of isotopic contamination and homogenization during which U and Pb were mobile.

(1) At about 1600 - 1800 My stratiform Cu-mineralizations became remobilized into vein deposits. Some of these discordant deposits also acquired high μ ratios and low κ ratios. The sulfide lead of the stratiform Cu-mineralizations and their host-rock, the basic metatuffs, was probably re-equilibrated, and the tuffs obtained U.

(2) At about 430 My, externally derived highly radiogenic lead was added to the sulfides of the various Fe- and Cu-mineralizations, as seen by mixing lines. Further, U was added to massive pyrrhotite mineralizations.

(3) The two events of isotopic disturbance are related to the Svecokarelian orogeny and the Caledonian orogeny. Both events resulted in metamorphism with the redistribution of lead and uranium. The generated fluids must have been sufficiently oxidized to transport U.

References

Adamek, P.M. 1975: Geology and mineralogy of the Koppar-åsen uraninite-sulphide mineralization, Norrbotten County, Sweden. *Sver. geol. under. Ser. C 712*, 67 pp.

Allégre, C.J., Dupré, B. & Lewin, E. 1986: Thorium/Uranium ratio of the earth. *Chem. Geol. 56*, 219—227.

Barnes, S.-J., Boyd, R., Korneliussen, A., Nilsson, L.-P., Often, M., Pederson, R.B. & Robins, B. (1988): The use of mantle normalization and metal ratios in discriminating between the effects of partial melting, crystal fractionation and sulphide segregation on the platinum-group elements, gold, nickel and copper: Examples from Norway. *In* Prichard, H.M., Potts, P.J., Bowles, J.F.W. & Cribb, S.J. (eds.) *Geoplatinum 87*, Elsevier, 113—143.

Bax, G. 1986: Basement involved Caledonian nappe tectonics in the Swedish part of the Rombak-Sjangeli window. *Geol. Fören. Förh. 108*, 268—270.

Bax, G. 1989: Caledonian structural evolution and tectono-stratigraphy in the Rombak-Sjangeli window and its covering sequences, Northern Scandinavian Caledonides. *Norges geol. unders. Bull.* (this volume).

Bergström, J. & Gee, D.G. 1985: The Cambrian in Scandinavia. *In* D.G. Gee and B.A. Sturt (eds.) *The Caledonian orogen — Scandinavia and related areas.* John Wiley & Sons Ltd., Chichester, 247—271.

Bird, D.K. & Helgeson, H.C. 1981: Chemical interaction of aqueous solutions with epidote-feldspar mineral assemblages in geologic systems. II Equilibrium constraints in metamorphic/geothermal processes. *Am. J. Sci. 281*, 576—614.

Boyle, R.W. 1982: *Geochemical prospecting for thorium and uranium deposits.* Developments in Economic geology 16. Elsevier, Amsterdam, 498 pp.

Bryhni, I. & Andreasson, P.-G. 1985: Metamorphism in the Scandinavia Caledonides. *In* D.G. Gee & B.A. Sturt (eds.) *The Caledonian orogen - Scandinavia and related areas.* John Wiley & Sons Ltd., Chichester, 763—781.

Cameron, A.E., Smith, D.H. & Walker, R.L. 1969: Mass spectrometry of nanogram-size samples of lead. *Analyt. Chem. 41*, 525—526.

Dostal, J. & Capedri, S. 1978: Uranium in metamorphic rocks. *Contrib. Mineral. Petrol. 66*, 409—414.

Gaál, G. & Gorbatschev, R. 1987: An outline of the Precambrian evolution of the Baltic Shield. *Precamb. Res. 35*, 15—52.

Gorbatschev, R. 1985: Precambrian basement of the Scandinavian Caledonides. *In* D.G. Gee & B.A. Sturt (eds.) *The Caledonian orogen - Scandinavia and related areas.* John Wiley & Sons, Chichester, 197—212.

Griffin, W.L., Taylor, P.N., Hakkinen, J.W., Heier, K.S., Iden, I.K., Krogh, E.J., Malm, O., Olsen, K.I., Ormaasen, D.E. & Tveten, E. 1978: Archaean and Proterozoic crustal evolution in Lofoten-Vesterålen, N Norway. *J. Geol. Soc. London 135*, 629—647.

Grünenfelder, M., Tilton, G.R., Bell, K. & Blenkinsop, J. 1986: Lead and strontium isotope relationships in the Oka carbonatite complex, Quebec. *Geochim. Cosmochim. Acta 50*, 461—468.

Gunner, J.D. 1981: A reconnaisance Rb-Sr study of Precambrian rocks from the Sjangeli-Rombak window and the pattern of initial ⁸⁷Sr/⁸⁶Sr ratios from northern Scandinavia. *Nor. Geol. Tidsskr. 61*, 281—290.

Heier, K.S. & Compston, W. 1969: Interpretation of Rb-Sr age patterns in high-grade metamorphic rocks, North Norway. *Nor. Geol. Tidsskr. 49*, 257—283.

Heier, K.S. & Thoresen, K. 1971: Geochemistry of high grade metamorphic rocks, Lofoten-Vesterålen, North Norway. *Geochim. Cosmochim. Acta 35*, 89—99.

Jacobsen, S. & Wasserburg, G.J. 1978: Interpretation of Nd, Sr and Pb isotope data from Archean migmatites *in* Lofoten-Vesterålen, Norway. *Earth Planet. Sci. Lett. 41*, 245—253.

Johansson, Å. 1983: Lead isotope composition of Caledonian sulfide-bearing veins in Sweden. *Econ. Geol. 78*, 1674—1688.

Korneliussen, A., Tollefsrud, J.I., Flood, B. & Sawyer, E. 1986: Precambrian volcano-sedimentary sequences and related ore deposits, with special reference to the Gautelisfjell carbonate-hosted, disseminated gold deposit, Rombaken basement window, Northern Norway. *Nor. geol. unders. Unpubl. report Nr. 86.193.*, 46 pp.

Kulling, O. 1964: Översikt över norra Norrbottensfjällens Kaledonberggrund, Karta Skala 1:400 000. *Sver. geol. unders. Ba 19*, 166 pp.

Langmuir, D. 1978: Uranium solution-mineral equilibria at low temperatures with applications to sedimentary ore deposits. *Geochim. Cosmochim. Actra 42*, 547—569.

Romberger, S.G. 1984: Transport and deposition of uranium in hyderothermal systems at temperatures up to 300°C: geological implications. *In* B. DeVivo, F. Ippolito, G. Capaldi & P.R. Simpson (eds.) *Uranium geochemistry, mineralogy, geology, exploration and resources.* Inst. Min. Metall., 12—17.

Romer, R.L. 1987: The geology, geochemistry and metamorphism of the Sjangeli area, a tectonic window in the Caledonides of northern Sweden. *Research Report Luleå University. TULEA 1987:16*, 124 pp.

Romer, R.L. 1989: Implications of isotope data on the metamorphism of the basic volcanites from the Sjangeli window, northern Sweden. *Norges geol. unders. Bull.* (this volume).

Skiöld, T. 1986: On the age of the Kiruna greenstones, northern Sweden. *Precamb. Res. 32*, 35—44.

Skiöld, T. 1987: Aspects of the Proterozoic geochronology of northern Sweden. *Precamb. Res. 35*, 161—167.

Stacey, J.S. & Kramers, J.D. 1975: Approximation of terrestrial lead isotope evolution by a two-stage model. *Earth Planet. Sci. Lett. 26*, 207—221.

Steiger, R.H. & Jäger, E. 1977: Subcommission on Geochronology: Convention on the use of decay constants in geo- and cosmochronology. *Earth Planet. Sci. Lett. 36*, 359—362.

Sundblad, K. & Røsholt, B. 1986: A lead isotopic study of galena and amazonite in the Kiuri-rassåive sulphide deposit — consequences for the timing of the ore forming processes in the Proterozoic of northernmost Sweden. *17:e Nordiska Geologmøtet, Helsinki, Abstr. vol.*, p. 196.

Todt, W., Cliff, R.A., Hanser, A. & Hofmann, A.W. 1984: ²⁰²Pb + ²⁰⁵Pb double spike for lead isotopic analyses. *Terra Cognita 4*, p. 209.

Tull, J.F., Bartley, J.M., Hodges, K.V., Andresen, A., Steltenpohl, M.G. & White, J.M. 1985: The caledonides in the Ofoten region (68° - 69°N), north Norway: key aspects of tectonic evolution. *In* D.G. Gee & B.A. Sturt (eds.) *The Caledonian orogen - Scandinavia and related areas.* John Wiley & Sons, Chichester, 553—568.

Vaasjoki, M. 1981: The lead composition of some Finnish galenas. *Geol. Surv. Finland Bull. 316*, 25 pp.

Vogt, T. 1950: Narvik, Berggrunnsgeologisk kart, 1:100 000. *Nor. geol. unders.*

Zartman, R.E. & Doe, B.R. 1981: Plumbotectonic — the model: *Tectonophysics 75*, 135—162.